Received: 14 March 2021 | Revised: 29 May 2021 | Accepted: 17 June 2021

DOI: 10.1002/ddr.21851

RESEARCH ARTICLE

DRUG DEVELOPMENT RESEARCH WILEY

Antibacterial and anti-inflammatory activity of valproic acid-pyrazole conjugates as a potential agent against periodontitis

Lei Dong[1] | Ling Fang[2] | Xinxiang Dai[3] | Jia Zhang[1] | Jia Wang[1] | Pei Xu[1]

[1]School of Stomatology, Anhui Medical College, Heifei, Anhui, China

[2]Department of Stomatology, Huangshan City People's Hospital Huangshan, Anhui, China

[3]Department of Stomatology, The Affiliated Anqing Hospital of Anhui Medical University, Anqing, Anhui, China

Correspondence
Lei Dong, Department of Stomatology, Anhui Medical College, Heifei, Anhui 230601, China.
Email: dlz999@sohu.com

Abstract

Periodontitis is a serious global concern. Therefore, in the present study, we intend to synthesize novel valproic-acid pyrazole conjugates as a novel agent against periodontitis. The molecules were developed in a facile synthetic route and obtained in excellent yields. The entire set of molecules were screened for antibacterial activity against a battery of micro-organisms responsible for periodontitis such as *P. gingivalis*, *P. intermedia*, *F. nucleatum*, and *E. coli*, where they exhibit considerable inhibitory activity. The most potent compound among the tested series, compound **7c** showed bactericidal activity in the time-kill curve against *E. coli*. Compound **7c** also showed inhibition of NF-κB transcriptional activity in LPS-stimulated RAW264.7 cells with IC_{50} of 19.23 μM. The effect of compound **7c** was also investigated in experimentally induced periodontitis in rats on various indices of oxidative stress (MDA, SOD, and GSH), inflammation (TNF-α, IL-1β, and IL-6), and apoptosis. It has been found that compound **7c** significantly inhibits oxidative stress, inflammation, and apoptosis in a dose-dependent manner. Compound **7c** also inhibits the expression of COX-2 and iNOS as shown by western blot analysis.

KEYWORDS

COX-2, hybrid compounds, RAW264.7 cells, synthesis

1 | INTRODUCTION

The food materials have made the oral cavity heaven for the growth of many microbial organisms which gives rise to several diseases. These oral diseases are observed mainly due to the development of numerous infections and inflammation [Wade, 2012]. Periodontal diseases are the major cause of oral inflammation which is responsible for inflammation of gingival tissues and irreversible loss of alveolar bone and ultimately loss of a tooth. It affects approximately 10–15% of the world population and thus needs immediate clinical interventions. The therapeutic modalities to treat periodontitis have been relying on reducing dental bacteria levels by scaling and root planning [Cekici et al., 2014]. Numerous studies have indicated the role of Gram-negative pathogens, for example, *Escherichia coli*, *Porphyromonas gingivalis*, *Prevotella intermedia*, *Actinobacillus*, and *Fusobacterium* sp in the progression of periodontal diseases. However, the antibiotics have lost their effectiveness due to the generation of resistance. On the other hand, infection-led inflammation in periodontitis worsens the disease [Hajishengallis, 2015; Li et al., 2000]. Therefore, newer therapies that concomitantly target both bacterial infections and inflammation are deemed suitable to treat periodontal diseases and can able to thwart the predicament faced by contemporary regimens.

Valproic acid is a well-known drug used to treat epilepsy via inhibition voltage-gated sodium channels. In recent studies, it reduces neuroinflammation following the traumatic injury via inhibition of histone deacetylase (HDCA) functions and inhibits the production of TNF-α and IL-6 and activation of NF-κB [Phiel et al., 2001; Diederich et al., 2010]. It also showed considerable antimicrobial activity against *P. aeruginosa* and *E. coli* [Zutz et al., 2016]. Pyrazole on another hand showed diverse pharmacological activities such as antiviral, antibacterial, anticancer, antimalarial, etc. Many pyrazole derivatives have already been used in clinical practice as potent nonsteroidal

anti-inflammatory drugs, such as celecoxib, antipyrine, metamizole, aminophenazone, phenylbutazone, sulfinpyrazone, and oxyphenbutazone. Some of the pyrazole derivatives showed potent inhibition of NF-κB [Karrouchi et al., 2018; Ansari et al., 2016; Khan et al., 2016]. Contemplating this evidence, we envisaged developing a single skeleton joining both valproic acid and pyrazole to search for novel agents against periodontitis. These molecules were tested for antibacterial activity, NF-κB inhibitory activity, and the effect of the most potent analog was examined into the animal model of periodontitis.

2 | EXPERIMENTAL

2.1 | Chemistry

All commercially available solvents and reagents were of analytical grade and used without further purification. Melting points were determined on a Veego, MPI melting point apparatus and FTIR (2.0 cm^{-1}, flat, smooth) was recorded on Perkin Elmer RX-I Spectrophotometer. ^{1}H NMR spectra were recorded in *d6*-DMSO on a Bruker Avance-400 NMR spectrometer with TMS as the internal reference. ^{13}C NMR spectra were recorded on a Bruker Avance-100 NMR spectrometer in *d6*-DMSO on the same spectrometers with TMS as the internal reference. Mass spectra were obtained on VG-AUTOSPEC spectrometer equipped with electrospray ionization (ESI) sources.

2.1.1 | Synthesis of methyl 2-propylpentanoate (2)

2-propyl pentanoic acid (**1**) (0.01 mol) was charged into 250 ml round bottom flask. 15 ml of methanol was added into above flask. 3–4 drops of Con. Sulfuric acid was added as a catalyst. The reaction mixture was refluxed for 12–14 h on water bath. The progress and the completion of the reaction were checked by silica gel-G F_{254} thin layer chromatography using hexane: ethyl acetate (4:6) as a mobile phase. After the completion of the reaction, excess of methanol was removed under reduced pressure. The separated product was extracted using ethyl acetate (30 ml × 3), the combined organic layer was washed using 5% sodium bicarbonate solution (20 ml × 2) followed by water (20 ml × 2). The organic layer was dried on anhydrous sodium sulfate and the solvent was removed under reduced pressure to acquire the product in a viscous liquid form. B.P. 170–172°C [Parekh, 2010].

2.1.2 | Synthesis of 2-propylpentanehydrazide (3)

Methyl 2-propylpentanoate (**2**) (0.01 mol) and 80% solution of hydrazine hydrate (52.5 g; 0.84 M) in ethanol (50 ml) were charged in the round bottom flask with 250 ml capacity. The mixture was refluxed on the water bath for 13–15 h. The reaction was monitored by TLC using hexane (4): ethyl acetate (6) as a mobile phase. Hydrazine hydrate was then removed at the bath temperature at 25°C. The ethanol was removed by rotary evaporation at bath temperature at 30°C. The ethanol–hydrazine mixture collected in a trapping flask can be used for the preparation of next portion of hydrazone. Cool the mixture at room temperature after completion of reaction to give the intermediate product (**3**) with 68% yield M. P.—124–126°C [Parekh, 2010].

2.1.3 | General procedure for the synthesis of substituted chalcone derivatives 6(a–h)

Various substituted acetophenone **4(a–h)**, (0.01 mol), and 4-hydroxybenzaldehyde (5) (0.01 mol) were dissolved in 40 ml of ethanol. Aqueous NaOH (0.05 mol) solution was added dropwise to the above mixture with stirring. The mixture was stirred at room temperature for 24 h. The reaction was monitored by TLC using n-butanol: acetic acid: water (4:3:1) as a mobile phase. The reaction mixture was poured into ice water after the completion of the reaction. The resulting product was precipitated, filtered, washed with water, dried, and recrystallized with ethanol to give substituted chalcone derivatives **6(a–h)** [UP Singh et al., 2012].

2.1.4 | 3-(4-Hydroxyphenyl)-1-phenylprop-2-en-1-one (6a)

Yield: 69%; B.p.: 108–109°C; MW: 224.26; R_f: 0.48; FTIR (v_{max}; cm^{-1} KBr): 3223.14 (O—H stretching), 3025.68 (Aromatic C—H stretching), 1723.36 (C═O stretching), 1637.42 (C═C stretching), 732; ^{1}H NMR (400 MHz, DMSO-*d6*, TMS) δ ppm: 9.28 (s, 1H, Ar—OH), 8.14 (d, 1H, $J = 7.98$ Hz, Ar—CH), 7.76 (d, 2H, $J = 1.92$ Hz, Ar—H), 7.57 (t, 1H, $J = 1.47$ Hz, Ar—H), 7.48 (d, 2H, $J = 1.53$ Hz, Ar—H), 7.42 (d, 2H, $J = 1.32$ Hz, Ar—H), 6.89 (d, 2H, $J = 1.68$ Hz, Ar—H), 6.62 (d, 1H, $J = 8.23$ Hz, CH); ^{13}C NMR (100 MHz, DMSO-*d6*) δ ppm:189.7 (C═O), 157.8 (C_4), 145.2 (Aliphatic CH_2), 137.8 (C'_1), 134.6 (C'_4), 130.5 (C_2,C_6), 129.3 (C'_5,C'_3), 128.5 (C'_2,C'_6), 127.8 (C_1), 121.3 (Aliphatic CH_2), 115.8 (C_3,C_5); (M + H)+; Elemental analysis for $C_{15}H_{12}O_2$: Calculated: C, 80.34; H, 5.39, O, 14.27. Found: C, 80.32; H, 5.37; O, 14.23.

2.1.5 | 1-(4-Chlorophenyl)-3-(4-hydroxyphenyl) prop-2-en-1-one (6b)

Yield: 84%; M.p: 189–190°C; MW: 258.70; R_f: 0.59; FTIR ($_{Vmax}$; cm^{-1} KBr): 3229.23 (O—H stretching), 3038.21 (Aromatic C—H stretching), 1721.39 (C═O stretching), 1632.41 (C═C stretching), 792.45 (C—Cl stretching), 723.67; ^{1}H NMR (400 MHz, DMSO-*d6*, TMS) δ ppm: 9.32 (s, 1H, Ar—OH), 8.09 (d, 1H, $J = 7.87$ Hz, Ar—CH), 7.58 (d, 2H, $J = 1.91$ Hz, Ar—H), 7.52 (d, 2H, $J = 1.38$ Hz, Ar—H), 7.45 (d, 2H, $J = 1.31$ Hz, Ar—H), 6.92 (d, 2H, $J = 1.71$ Hz, Ar—H), 6.67 (d, 1H, $J = 8.42$ Hz, CH); ^{13}C NMR (100 MHz, DMSO-*d6*) δ ppm:189.6 (C═O), 157.8 (C_4), 145.1(Aliphatic CH_2), 140.3 (C'_4), 136.2 (C'_1), 130.6

(C_2,C_6), 130.2 (C'_2,C'_6), 129.3 (C'_5,C'_3), 127.8 (C_1), 121.3 (Aliphatic CH_2), 115.8 (C_3,C_5); (M + H)+; Elemental analysis for $C_{15}H_{11}ClO_2$: Calculated: C, 69.64; H, 4.29; O, 12.37. Found: C, 69.58; H, 4.34; O, 12.41.

2.1.6 | 1-(4-Fluorophenyl)-3-(4-hydroxyphenyl) prop-2-en-1-one (6c)

Yield: 78%; M.p: 185–186°C; MW: 242.25; R_f: 0.53; FTIR (ν_{max}; cm^{-1} KBr): 3234.19 (O—H stretching), 3019.26 (Aromatic C—H stretching), 1718.31 (C=O stretching), 1628.39 (C=C stretching), 1159.34 (C—F stretching), 729.61; ^{1}H NMR (400 MHz, DMSO-*d6*, TMS) δ ppm: 9.34 (s, 1H, Ar—OH), 8.04 (d, 1H, *J* = 7.87 Hz, Ar—CH), 7.65 (d, 2H, *J* = 1.84 Hz, Ar—H), 7.54 (d, 2H, *J* = 1.91 Hz, Ar—H), 7.39 (d, 2H, *J* = 1.04 Hz, Ar—H), 6.89 (d, 2H, *J* = 1.75 Hz, Ar—H), 6.65 (d, 1H, *J* = 8.38 Hz, CH); ^{13}C NMR (100 MHz, DMSO-*d6*) δ ppm:189.5 (C=O), 168.9 (C'_4), 157.8 (C_4), 145.3 (Aliphatic CH_2), 133.5 (C'_1), 131.8 (C'_2,C'_6), 130.2 (C_2,C_6), 127.5 (C_1), 121.4 (Aliphatic CH_2), 116.1 (C'_5,C'_3), 115.2 (C_3,C_5); (M + H)+; Elemental analysis for $C_{15}H_{11}FO_2$: Calculated: C, 74.37; H, 4.58; O, 13.21. Found: C, 74.40; H, 4.58; O, 13.18.

2.1.7 | 1-(4-Bromophenyl)-3-(4-hydroxyphenyl) prop-2-en-1-one (6d)

Yield: 84%; M.p: 167–168°C; MW: 303.16; R_f: 0.59; FTIR (ν_{max}; cm^{-1} KBr): 3239.24 (O—H stretching), 3023.17 (Aromatic C—H stretching), 1715.37 (C=O stretching), 1623.31 (C=C stretching), 1493.48 (C—Br stretching), 723.69; ^{1}H NMR (400 MHz, DMSO-*d6*, TMS) δ ppm: 9.32 (s, 1H, Ar—OH), 8.07 (d, 1H, *J* = 7.82 Hz, Ar—CH), 7.84 (d, 2H, *J* = 1.81 Hz,Ar—H), 7.67 (d, 2H, *J* = 1.35 Hz, Ar—H), 7.52 (d, 2H, *J* = 1.89 Hz, Ar—H), 6.87 (d, 2H, *J* = 1.72 Hz, Ar—H), 6.69 (d, 1H, *J* = 8.49 Hz, CH); ^{13}C NMR (100 MHz, DMSO-*d6*) δ ppm:189.8 (C=O), 157.9 (C_4), 145.3(Aliphatic CH_2), 136.9 (C'_1), 132.2 (C'_5,C'_3), 130.8 (C_2,C_6), 130.1 (C'_2,C'_6), 128.7 (C'_4), 127.9 (C_1), 121.4 (Aliphatic CH_2), 115.8 (C_3,C_5); Mass: 304.16 (M + H)+; Elemental analysis for $C_{15}H_{11}BrO_2$: Calculated: C, 59.43; H, 3.66; O, 10.55. Found: C, 59.48; H, 3.64; O, 10.57.

2.1.8 | 3-(4-Hydroxyphenyl)-1-(p-tolyl)prop-2-en-1-one (6e)

Yield: 69%; M.p: 175–176°C; MW: 238.29; R_f: 0.72; FTIR (ν_{max}; cm^{-1} KBr): 3242.15 (O—H stretching), 3025.12 (Aromatic C—H stretching), 2954.63 (alkyl C—H stretching), 1719.31 (C=O stretching), 1628.43 (C=C stretching), 1465.82 (CH3 bending), 727.62; ^{1}H NMR (400 MHz, DMSO-*d6*, TMS) δ ppm: 9.38 (s, 1H, Ar—OH), 8.04 (d, 1H, *J* = 7.89 Hz, Ar—CH), 7.79 (d, 2H, *J* = 1.76 Hz, Ar—H), 7.56 (d, 2H, *J* = 1.91 Hz, Ar—H), 7.14 (d, 2H, *J* = 1.23 Hz, Ar—H), 6.91 (d, 2H, *J* = 1.68 Hz, Ar—H), 6.67 (d, 1H, *J* = 8.37 Hz, CH), 2.31 (s, 3H, CH_3); ^{13}C NMR (100 MHz, DMSO-*d6*) δ ppm:189.5 (C=O), 157.9 (C_4), 145.3 (Aliphatic CH_2), 144.4 (C'_4), 134.8 (C'_1), 130.8 (C_2,C_6), 129.8 (C'_2,C'_6), 129.2 (C'_5,C'_3), 127.8 (C_1), 121.4 (Aliphatic CH_2), 115.9 (C_3, C_5), 21.4 (CH_3); Mass: 239.30 (M + H)+; Elemental analysis for $C_{16}H_{14}O_2$: Calculated: C, 80.65; H, 5.92; O, 13.43. Found: C, 80.62; H, 5.93; O, 13.43.

2.1.9 | 3-(4-Hydroxyphenyl)-1-(4-methoxyphenyl) prop-2-en-1-one (6f)

Yield: 85%; M.p: 158–158°C; MW: 254.29; R_f: 0.63; FTIR (ν_{max}; cm^{-1} KBr): 3245.12 (O—H stretching), 3029.52 (Aromatic C—H stretching), 2823.72 (OCH_3 stretching), 1714.65 (C=O stretching), 1623.49 (C=C stretching), 723.58; ^{1}H NMR (400 MHz, DMSO-*d6*, TMS) δ ppm: 9.34 (s, 1H, Ar—OH), 8.02 (d, 1H, *J* = 7.79 Hz, Ar—CH), 7.87 (d, 2H, *J* = 1.82 Hz, Ar—H), 7.54 (d, 2H, *J* = 1.93 Hz, Ar—H), 7.08 (d, 2H, *J* = 1.21 Hz, Ar—H), 6.87 (d, 2H, *J* = 1.74 Hz, Ar—H), 6.69 (d, 1H, *J* = 8.42 Hz, CH), 3.87 (s, 3H, OCH_3); ^{13}C NMR (100 MHz, DMSO-*d6*) δ ppm:189.5 (C=O), 166.8 (C'_4), 157.9 (C_4), 145.3 (Aliphatic CH_2), 131.2 (C'_2,C'_6), 130.8 (C_2,C_6), 130.2 (C'_1), 127.8 (C_1), 121.4 (Aliphatic CH_2), 115.8 (C_3, C_5), 114.9 (C'_3,C'_5), 55.8 (OCH_3); Mass: 255.28 (M + H)+; Elemental analysis for $C_{16}H_{14}O_3$: Calculated: C, 75.58; H, 5.55; O, 18.88. Found: C, 75.56; H, 5.58; O, 18.90.

2.1.10 | 3-(4-Hydroxyphenyl)-1-(4-nitrophenyl) prop-2-en-1-one (6 g)

Yield: 71%; M.p: 184–185°C; MW: 269.26; R_f: 0.51; FTIR (ν_{max}; cm^{-1} KBr): 3248.16 (O—H stretching), 3024.47 (Aromatic C—H stretching), 1719.51 (C=O stretching), 1628.43 (C=C stretching), 1537.92 (NO2 stretching), 727.52; ^{1}H NMR (400 MHz, DMSO-*d6*, TMS) δ ppm: 9.37 (s, 1H, Ar—OH), 8.14 (d, 2H, *J* = 1.87 Hz,Ar—H), 8.04 (d, 1H, *J* = 7.73 Hz, Ar—CH), 7.86 (d, 2H, *J* = 1.52 Hz, Ar—H), 7.56 (d, 2H, *J* = 1.92 Hz, Ar—H), 6.92 (d, 2H, *J* = 1.63 Hz, Ar—H), 6.65 (d, 1H, *J* = 8.58 Hz, CH); ^{13}C NMR (100 MHz, DMSO-*d6*) δ ppm:189.9 (C=O), 157.8 (C_4), 153.4 (C'_4), 145.2 (Aliphatic CH_2), 144.3 (C'_1), 130.9 (C'_2,C'_6), 130.2 (C_2,C_6), 127.9 (C_1), 124.6 (C'_3,C'_5), 121.4 (Aliphatic CH_2), 115.9 (C_3, C_5); Mass: 270.25 (M + H)+; Elemental analysis for $C_{15}H_{11}NO_4$: Calculated: C, 66.91; H, 4.12; N, 5.20; O, 23.77. Found: C, 66.95; H, 4.12; N, 5.21; O, 23.80.

2.1.11 | 1,3-Bis(4-hydroxyphenyl)prop-2-en-1-one (6 h)

Yield: 87%; M.p: 135–137°C; MW: 240.26; R_f: 0.43; FTIR (ν_{max}; cm^{-1} KBr): 3241.12 (O—H stretching), 3029.43 (Aromatic C—H stretching), 1714.62 (C=O stretching), 1625.49 (C=C stretching), 732.48; ^{1}H NMR (400 MHz, DMSO-*d6*, TMS) δ ppm: 9.42 (s, 2H, Ar—OH), 8.07 (d, 1H, *J* = 8.92 Hz,Ar—CH), 7.57 (d, 2H, *J* = 1.78 Hz, Ar—H), 7.54 (d, 2H, *J* = 1.91 Hz, Ar—H), 6.89 (d, 2H, *J* = 1.72 Hz, Ar—H), 6.86 (d, 2H,

J = 1.09 Hz, Ar—H), 6.68 (d, 1H, J = 8.52 Hz, CH); ^{13}C NMR (100 MHz, DMSO-*d6*) δ ppm:189.3(C═O), 164.6 (C'_4), 157.8 (C_4), 145.2 (Aliphatic CH_2), 131.4 (C'_2,C'_6), 130.8 (C_2,C_6), 130.1 (C'_1), 127.9 (C_1), 121.4 (Aliphatic CH_2), 116.5 (C'_3,C'_5), 115.8 (C_3,C_5); Mass: 241.26 (M + H)+; Elemental analysis for $C_{15}H_{12}O_3$: Calculated: C, 74.99; H, 5.03; O, 19.98. Found: C, 74.97; H, 5.02; O, 19.96.

2.1.12 | General procedure for the synthesis of title compounds 7(a–h)

Substituted chalcone derivatives **6(a–h)** (0.01 mol) were dissolved in 20 ml of ethanol in 250 ml of the bottom flask, and 2-propyl pentanohydrazide (**3**) (0.01 mol) was added to the above solution. The mixture was refluxed on the water bath for 14–15 h in presence of 1 ml of NaOH solution. The reaction was monitored by TLC by using the appropriate solvent as the mobile phase. The reaction mixture was poured into ice water after the completion of the reaction. The resulting product was precipitated, filtered, washed with water, dried, and recrystallized with ethanol to give title compounds **7(a-h)**.

2.1.13 | 1-(5-(4-Hydroxyphenyl)-3-phenyl-4,5-dihydro-1H-pyrazol-1-yl)-2-propylpentan-1-one (7a)

Yield: 84%; M.p: 204–205°C; MW: 364.49; R_f: 0.73; FTIR ($_{Vmax}$; cm^{-1} KBr): 3258.18 (O—H stretching), 3026.42 (Aromatic C—H stretching), 2967.45 (CH_3 stretching), 2938.27 (CH2 stretching), 2854.81 (CH_3 stretching), 1719.34 (C═O stretching), 1674.36 (C═N stretching), 1529.82 (C═C stretching), 1389.93 (N—N stretching), 739.41; ^{1}H NMR (400 MHz, DMSO-*d6*, TMS) δ ppm: 9.05 (s, 1H, Ar—OH), 8.35 (d, 2H, J = 7.93 Hz,Ar—H), 7.42 (d, 2H, J = 1.86 Hz, Ar—H), 7.28 (t, 1H, J = 1.30 Hz, Ar—H), 7.21 (d, 2H, J = 1.03 Hz, Ar—H), 6.65 (d, 2H, J = 2.06 Hz, Ar—H), 5.63 (d, 1H, J = 4.28 Hz, pyrazole-H), 3.14 (d, 2H, J = 8.06 Hz, pyrazole-H), 2.39 (q, 1H, J = 7.57 Hz, CH), 1.49–0.89 (m, 14H, aliphatic-H); ^{13}C NMR (100 MHz, DMSO-*d6*) δ ppm:176.9 (C═O), 156.5 (C_4), 151.8 (Pyrazole C_3), 136.4 (C'_1), 134.3 (C_1), 131.1 (C'_4), 128.9 (C'_3,C'_5), 128.1 (C'_2,C'_6), 127.0 (C_2,C_6), 115.8 (C_3,C_5), 66.7 (Pyrazole C_5), 44.1 (CH), 39.8 (Pyrazole C_4), 35.5 (Aliphatic C_1, C_3), 20.4 (Aliphatic C_2,C_4), 14.1 (CH_3); Mass: 365.48 (M + H)+; Elemental analysis for $C_{23}H_{28}N_2O_2$: Calculated: C, 75.79; H, 7.74; N, 7.69; O, 8.78. Found: C, 75.86; H, 7.75; N, 7.65; O, 8.79.

2.1.14 | 1-(3-(4-Chlorophenyl)-5-(4-hydroxyphenyl)-4,5-dihydro-1H-pyrazol-1-yl)-2-propylpentan-1-one (7b)

Yield: 72%; M.p: 212–213°C; MW: 398.93; R_f: 0.53; FTIR ($_{Vmax}$; cm^{-1} KBr): 3264.12 (O—H stretching), 3021.49 (Aromatic C—H stretching), 2964.47 (CH3 stretching), 2932.23 (CH2 stretching), 2851.87 (CH3 stretching), 1713.38 (C═O stretching), 1672.43 (C═N stretching), 1528.84 (C═C stretching), 1386.92 (N—N stretching), 793.62 (C—Cl stretching), 732.49; ^{1}H NMR (400 MHz, DMSO-*d6*, TMS) δ ppm: 9.07 (s, 1H, Ar—OH), 7.68 (d, 2H, J = 7.38 Hz,Ar—H), 7.38 (d, 2H, J = 1.89 Hz, Ar—H), 7.25 (d, 2H, J = 1.05 Hz, Ar—H), 6.68 (d, 2H, J = 2.09 Hz, Ar—H), 5.67 (d, 1H, J = 4.32 Hz, pyrazole-H), 3.21 (d, 2H, J = 8.02 Hz, pyrazole-H), 2.42 (q, 1H, J = 7.64 Hz, CH), 1.52–0.90 (m, 14H, aliphatic-H); ^{13}C NMR (100 MHz, DMSO-*d6*) δ ppm:176.4 (C═O), 156.3 (C_4), 151.9 (Pyrazole C_3), 136.8 (C'_4), 134.7 (C'_1), 134.1 (C_1), 128.7 (C'_3,C'_5), 128.2 (C'_2,C'_6), 127.2 (C_2,C_6), 115.8 (C_3,C_5), 66.8 (Pyrazole C_5), 44.2 (CH), 39.8 (Pyrazole C_4), 35.6 (Aliphatic C_1, C_3), 20.5 (Aliphatic C_2,C_4), 14.3 (CH_3); Mass: 399.95 (M + H)+; Elemental analysis for $C_{23}H_{27}ClN_2O_2$: Calculated: C, 69.25; H, 6.82; N, 7.02; O, 8.02. Found: C, 69.24; H, 6.85; N, 7.04; O, 8.03.

2.1.15 | 1-(3-(4-Fluorophenyl)-5-(4-hydroxyphenyl)-4,5-dihydro-1H-pyrazol-1-yl)-2-propylpentan-1-one (7c)

Yield: 79%; M.p: 198–199°C; MW: 382.48; R_f: 0.43; FTIR ($_{Vmax}$; cm^{-1} KBr): 3267.19 (O—H stretching), 3024.42 (Aromatic C—H stretching), 2968.72 (CH3 stretching), 2934.21 (CH2 stretching), 2858.94 (CH3 stretching), 1723.19 (C═O stretching), 1675.41 (C═N stretching), 1524.81 (C═C stretching), 1389.72 (N—N stretching), 1163.76 (C—F stretching), 748.24; ^{1}H NMR (400 MHz, DMSO-*d6*, TMS) δ ppm: 9.24 (s, 1H, Ar—OH), 7.59 (d, 2H, J = 7.32 Hz,Ar—H), 7.25 (d, 2H, J = 1.06 Hz, Ar—H), 7.14 (d, 2H, J = 1.35 Hz, Ar—H), 6.63 (d, 2H, J = 2.04 Hz, Ar—H), 5.71 (d, 1H, J = 4.28 Hz, pyrazole-H), 3.26 (d, 2H, J = 8.09 Hz, pyrazole-H), 2.41 (q, 1H, J = 7.58 Hz, CH), 1.50–0.92 (m, 14H, aliphatic-H); ^{13}C NMR (100 MHz, DMSO-*d6*) δ ppm:178.2 (C═O), 166.3 (C'_4), 157.4 (C_4), 152.8 (Pyrazole C_3), 134.5 (C_1), 132.2 (C'_1), 129.7 (C'_2,C'_6), 127.1 (C_2,C_6), 115.9 (C_3,C_5), 115.4 (C'_3,C'_5), 66.7 (Pyrazole C_5), 44.2 (CH), 39.8 (Pyrazole C_4), 35.5 (Aliphatic C_1,C_3), 21.4 (Aliphatic C_2,C_4), 15.2 (CH_3); Mass: 383.47 (M + H)+; Elemental analysis for $C_{23}H_{27}FN_2O_2$: Calculated: C, 72.23; H, 7.12; N, 7.32; O, 8.37. Found: C, 72.28; H, 7.08; N, 7.34; O, 8.37.

2.1.16 | 1-(3-(4-Bromophenyl)-5-(4-hydroxyphenyl)-4,5-dihydro-1H-pyrazol-1-yl)-2-propylpentan-1-one (7d)

Yield: 74%; M.p: 234–236°C; MW: 443.39; R_f: 0.67; FTIR ($_{Vmax}$; cm^{-1} KBr): 3273.08 (O—H stretching), 3029.41 (Aromatic C—H stretching), 2962.84 (CH_3 stretching), 2932.17 (CH_2 stretching), 2853.75 (CH_3 stretching), 1719.08 (C═O stretching), 1678.38 (C═N stretching), 1529.63 (C═C stretching), 1384.71 (N—N stretching), 763.48 (C—Br stretching), 751.12; ^{1}H NMR (400 MHz, DMSO-*d6*, TMS) δ ppm: 9.15 (s, 1H, Ar—OH), 7.52 (d, 2H, J = 7.28 Hz,Ar—H), 7.49 (d, 2H, J = 1.89 Hz, Ar—H), 7.21 (d, 2H, J = 1.05 Hz, Ar—H), 6.68 (d, 2H, J = 2.09 Hz, Ar—H), 5.63 (d, 1H, J = 4.23 Hz, pyrazole-H), 3.12 (d, 2H, J = 8.03 Hz, pyrazole-H), 2.45 (q, 1H, J = 7.53 Hz, CH), 1.51–0.88 (m, 14H, aliphatic-H); ^{13}C NMR (100 MHz, DMSO-*d6*) δ ppm:179.2

(C═O), 158.4 (C_4), 154.5 (Pyrazole C_3), 136.2 (C'_1), 134.4 (C_1), 131.9 (C'_3,C'_5), 128.6 (C'_2,C'_6), 127.2 (C_2,C_6), 125.2 (C'_4), 115.9 (C_3,C_5), 66.2 (Pyrazole C_5), 45.2 (CH), 39.7 (Pyrazole C_4), 35.3 (Aliphatic C_1,C_3), 20.5 (Aliphatic C_2,C_4), 15.2 (CH_3); Mass: 444.39 (M + H)+; Elemental analysis for $C_{23}H_{27}BrN_2O_2$: Calculated: C, 62.31; H, 6.14; N, 6.32; O, 7.22. Found: C, 62.37; H, 6.18; N, 6.31; O, 7.19.

2.1.17 | 1-(5-(4-Hydroxyphenyl)-3-(p-tolyl)-4,5-dihydro-1H-pyrazol-1-yl)-2-propylpentan-1-one (7e)

Yield: 68%; M.p: 241–242°C; MW: 378.52; R_f: 0.51; FTIR (ν_{max}; cm^{-1} KBr): 3269.23 (O—H stretching), 3025.47 (Aromatic C—H stretching), 2961.87 (CH3 stretching), 2938.12 (CH_2 stretching), 2863.82 (CH_3 stretching), 1715.04 (C═O stretching), 1675.32 (C═N stretching), 1523.61 (C═C stretching), 1388.79 (N—N stretching), 743.15; ^{1}H NMR (400 MHz, DMSO-*d6*, TMS) δ ppm: 9.12 (s, 1H, Ar—OH), 7.49 (d, 2H, *J* = 7.34 Hz,Ar—H), 7.21 (d, 2H, *J* = 1.04 Hz, Ar—H), 7.13 (d, 2H, *J* = 1.27 Hz, Ar—H), 6.63 (d, 2H, *J* = 2.05 Hz, Ar—H), 5.69 (d, 1H, *J* = 4.29 Hz, pyrazole-H), 3.23 (d, 2H, *J* = 8.09 Hz, pyrazole-H), 2.42 (q, 1H, *J* = 7.58 Hz, CH), 2.24 (s, 3H, CH3), 1.53–0.92 (m, 14H, aliphatic-H); ^{13}C NMR (100 MHz, DMSO-*d6*) δ ppm:179.2 (C═O), 157.8 (C_4), 152.1 (Pyrazole C_3), 140.9 (C'_4), 134.6 (C_1), 133.7 (C'_1), 129.1 (C'_3. C'_5), 127.9 (C'_2,C'_6), 127.2 (C_2,C_6), 115.8 (C_3,C_5), 68.2 (Pyrazole C_5), 45.3 (CH), 39.8 (Pyrazole C_4), 35.6 (Aliphatic C_1,C_3), 21.4 (CH_3), 20.5 (Aliphatic C_2,C_4), 14.3 (CH_3); Mass: 379.51 (M + H) +; Elemental analysis for $C_{24}H_{30}N_2O_2$: Calculated: C, 76.16; H, 7.99; N, 7.40; O, 8.45. Found: C, 76.19; H, 8.02; N, 7.42; O, 8.46.

2.1.18 | 1-(5-(4-Hydroxyphenyl)-3-(4-methoxyphenyl)-4,5-dihydro-1H-pyrazol-1-yl)-2-propylpentan-1-one (7f)

Yield: 75%; M.p: 252–253°C; MW: 394.52; R_f: 0.54; FTIR (ν_{max}; cm^{-1} KBr): 3265.29 (O—H stretching), 3024.41 (Aromatic C—H stretching), 2967.82 (CH_3 stretching), 2932.11 (CH_2 stretching), 2868.84 (CH_3 stretching), 2832.47 (OCH_3 stretching), 1718.09 (C═O stretching), 1678.35 (C═N stretching), 1524.69 (C═C stretching), 1385.72 (N—N stretching), 748.12; ^{1}H NMR (400 MHz, DMSO-*d6*, TMS) δ ppm: 9.23 (s, 1H, Ar—OH), 7.45 (d, 2H, *J* = 7.82 Hz,Ar—H), 7.28 (d, 2H, *J* = 1.08 Hz, Ar—H), 7.23 (d, 2H, *J* = 1.05 Hz, Ar—H), 6.69 (d, 2H, *J* = 2.06 Hz, Ar—H), 5.67 (d, 1H, *J* = 4.23 Hz, pyrazole-H), 3.14 (d, 2H, *J* = 8.02 Hz, pyrazole-H), 3.82 (s, 3H, OCH3), 2.42 (q, 1H, *J* = 7.58 Hz, CH), 1.52–0.89 (m, 14H, aliphatic-H); ^{13}C NMR (100 MHz, DMSO-*d6*) δ ppm:178.9 (C═O), 162.8 (C'_4), 158.6 (C_4), 152.8 (Pyrazole C_3), 135.2 (C_1), 128.9 (C'_2,C'_6), 127.8 (C'_1), 127.1 (C_2, C_6), 115.9 (C_3,C_5), 114.8 (C'_3,C'_5), 67.8 (Pyrazole C_5), 55.9 (OCH_3), 45.2 (CH), 39.7 (Pyrazole C_4), 35.7 (Aliphatic C_1,C_3), 21.1 (Aliphatic C_2, C_4), 14.8 (CH_3); Mass: 395.52 (M + H)+; Elemental analysis for $C_{24}H_{30}N_2O_3$: Calculated: C, 73.07; H, 7.67; N, 7.10; O, 12.17. Found: C, 73.04; H, 7.79; N, 7.12; O, 12.19.

2.1.19 | 1-(5-(4-Hydroxyphenyl)-3-(4-nitrophenyl)-4,5-dihydro-1H-pyrazol-1-yl)-2-propylpentan-1-one (7 g)

Yield: 81%; M.p: 264–265°C; MW: 409.49; R_f: 0.59; FTIR (ν_{max}; cm^{-1} KBr): 3269.21 (O—H stretching), 3028.36 (Aromatic C—H stretching), 2963.87 (CH_3 stretching), 2935.18 (CH_2 stretching), 2862.83 (CH_3 stretching), 1714.08 (C═O stretching), 1675.32 (C═N stretching), 1537.52 (NO_2 stretching), 1527.62 (C═C stretching), 1389.76 (N—N stretching), 742.18; ^{1}H NMR (400 MHz, DMSO-*d6*, TMS) δ ppm: 9.26 (s, 1H, Ar—OH), 8.10 (d, 2H, *J* = 7.87 Hz,Ar—H), 7.61 (d, 2H, *J* = 1.92 Hz, Ar—H), 7.22 (d, 2H, *J* = 1.28 Hz, Ar—H), 6.64 (d, 2H, *J* = 2.08 Hz, Ar—H), 5.78 (d, 1H, *J* = 4.29 Hz, pyrazole-H), 3.23 (d, 2H, *J* = 8.07 Hz, pyrazole-H), 2.38 (q, 1H, *J* = 7.56 Hz, CH), 1.50–0.87 (m, 14H, aliphatic-H); ^{13}C NMR (100 MHz, DMSO-*d6*) δ ppm:179.1 (C═O), 158.6 (C_4), 152.3 (Pyrazole C_3), 150.2 (C'_4), 142.7 (C'_1), 134.5 (C_1), 128.1 (C_2,C_6), 127.9 (C'_2,C'_6), 127.1 (C'_3,C'_5), 115.9 (C_3,C_5), 66.8 (Pyrazole C_5), 44.3 (CH), 39.8 (Pyrazole C_4), 35.5 (Aliphatic C_1,C_3), 20.6 (Aliphatic C_2,C_4), 14.2 (CH_3); Mass: 410.50 (M + H)+; Elemental analysis for $C_{23}H_{27}N_3O_4$: Calculated: C, 67.46; H, 6.65; N, 10.26; O, 15.63. Found: C, 67.51; H, 6.65; N, 10.29; O, 15.61.

2.1.20 | 1-(3,5-Bis(4-hydroxyphenyl)-4,5-dihydro-1H-pyrazol-1-yl)-2-propylpentan-1-one (7 h)

Yield: 68%; M.p: 272–273°C; MW: 380.49; R_f: 0.62; FTIR (ν_{max}; cm^{-1} KBr): 3273.23 (O—H stretching), 3025.32 (Aromatic C—H stretching), 2968.82 (CH_3 stretching), 2939.17 (CH_2 stretching), 2864.85 (CH_3 stretching), 1718.09 (C═O stretching), 1678.35 (C═N stretching), 1529.61 (C═C stretching), 1386.72 (N—N stretching), 741.15; ^{1}H NMR (400 MHz, DMSO-*d6*, TMS) δ ppm: 9.32 (s, 2H, Ar—OH), 7.42 (d, 2H, *J* = 7.81 Hz, Ar—H), 7.24 (d, 2H, *J* = 1.05 Hz, Ar—H), 7.18 (d, 2H, *J* = 1.58 Hz, Ar—H), 6.67 (d, 2H, *J* = 2.03 Hz, Ar—H), 5.69 (d, 1H, *J* = 4.21 Hz, pyrazole-H), 3.21 (d, 2H, *J* = 8.03 Hz, pyrazole-H), 2.42 (q, 1H, *J* = 7.59 Hz, CH), 1.54–0.91 (m, 14H, aliphatic-H); ^{13}C NMR (100 MHz, DMSO-*d6*) δ ppm:178.2 (C═O), 160.9 (C'_4), 157.5 (C_4), 152.2 (Pyrazole C_3), 134.5 (C_1), 129.1 (C'_2,C'_6), 128.9 (C'_1), 127.1 (C_2, C_6) 116.1 (C'_3,C'_5), 115.8 (C_3,C_5), 66.7 (Pyrazole C_5), 45.2 (CH), 39.8 (Pyrazole C_4), 35.4 (Aliphatic C_1,C_3), 20.4 (Aliphatic C_2,C_4), 14.3 (CH_3); Mass: 381.48 (M + H)+; Elemental analysis for $C_{23}H_{28}N_2O_3$: Calculated: C, 72.60; H, 7.42; N, 7.36; O, 12.61. Found: C, 72.64; H, 7.40; N, 7.37; O, 12.58.

2.1.21 | In vitro NF-κB transcription inhibitory activity

The NF-κB transcription inhibitory activity of compound **7c** was performed in RAW264.7 macrophages obtained from ATCC, USA. The inhibitory activity was measured using an earlier reported procedure via employing Dual-Luciferase Reporter Assay System (Promega) according to the manufacturer's instructions [Srivastava, Awatade, et al., 2015].

2.1.22 | Animal experiments

The male Wistar rats (220–250 g) were obtained from an institutional animal house and kept in strict hygienic conditions with alternate light and dark cycles of 12 h at ambient temperature and humidity. The animals were supplied with a standard laboratory diet and water ad libitum. The study was approved by the Institutional Animal Ethics Committee of Anhui Medical College.

2.1.23 | Endotoxin preparation

To generate the endotoxin necessary for the animal experimentation, *E. coli* was cultivated on nutrient agar for the night to get the optimum colony count. The bacterial culture was then rinsed with PBS and the resulting liquid was mixed thoroughly phenol in a separating funnel. The aqueous phase was collected and extracted after washing thrice with phenol and supernatant was precipitated using ethanol and sodium acetate. The precipitate containing endotoxin was readily isolated by centrifugation at 10,000 g for 10 min and air-dried.

2.1.24 | Experimental periodontitis generation

The induced experimental periodontitis (EP), rats were received intragingival injection of 1 mg endotoxin dissolved in 1 ml saline into the labial and palatal aspects of the maxillary anterior gingivae and buccal cavity.

The rats were grouped in five groups (n = 6) as follows.

Group 1: control group.

Group 2: endotoxin only.

Group 3, 4 and 5: compound **7c** (5, 10, 20 mg/kg), respectively.

The compound **7c** was administered to rats once a day for total 6 days of the experimental period via oral intubation. The animals were killed after the end of the experiment by cervical decapitation under light ether anesthesia, and bone and teeth of the right maxillary halves were dissected out and used for further biochemical analysis.

2.1.25 | TUNEL staining for apoptosis determination

The gingival tissues were subjected to a TUNEL apoptosis detection kit (Wuhan Boster Biological Engineering Co., Ltd., Wuhan, China) according to the manufacturer's instruction.

2.1.26 | Estimation of biochemical mediators of oxidative stress

The level of MDA, GSH, and SOD was determined by commercially available ELISA (Jiangsu Enzyme Free Experimental Co., Ltd. China) kits as per the manufacturer protocol.

2.1.27 | Estimation of proinflammatory cytokines

The level of TNF-α, IL-1β, and IL-6 were determined in gingival samples by commercially available ELISA kits as per the manufacturer protocol (Jiangsu Enzyme Free Experimental Co., Ltd. China).

2.1.28 | Western blotting

The protein extract (30 μg) was resolved by 12% SDS-PAGE electrophoresis and electrotransferred onto a membrane of nitrocellulose. The membrane was blocked-up using TrisPBS (TPBS) with Tween 20 and 5% skimmed milk and probed with primary antibodies: Next, the secondary antibody conjugated to HRP (1: 10 000; Abcam/Cell Signaling Technology) in TPBS was added and incubated at 37°C for 1 h. Bands were visualized using an enhanced chemiluminescence image analyzer, and protein levels were quantified using Image-Pro Plus software (Media Cybernetics, Inc., MD, USA).

2.1.29 | Statistical analyses

All data are presented as the means ± *SD*. The results were analyzed with a one-way analysis of variance and the Bonferroni multiple range post hoc tests using the statistical software GraphPad Prism ver. 5.0 (CA, USA). P values below 0.05 were considered statistically.

3 | RESULTS AND DISCUSSION

3.1 | Chemistry

The synthesis of the title derivatives was outlined in Scheme 1. Initially, the synthesis has been started with the development of valproic acid utilizing 2-propyl pentanoic acid (**1**) as starting material to afford methyl 2-propylpentanoate (**2**). Compound **2** was further allowed to react to hydrazine to furnish the corresponding hydrazide derivative (**3**). The subsequent step corresponds to the development of numerous chalcone derivatives **6 (a–h)** by condensing 4-hydroxy benzaldehyde with corresponding acetophenone derivative **4 (a–h)**. The last step signifies the development of target derivatives **7** (**a–h**) via the cyclo-condensation reaction between compound **3** with corresponding **6** (**a–h**). The structures of compounds were ascertained via analytical and spectroscopic techniques (^{1}H-NMR, ^{13}C-NMR, mass, and elemental analysis).

3.2 | Pharmacological activity

3.2.1 | Antibacterial activity

The synthesized compounds were screened for antibacterial activity against a battery of micro-organism responsible for periodontitis. The

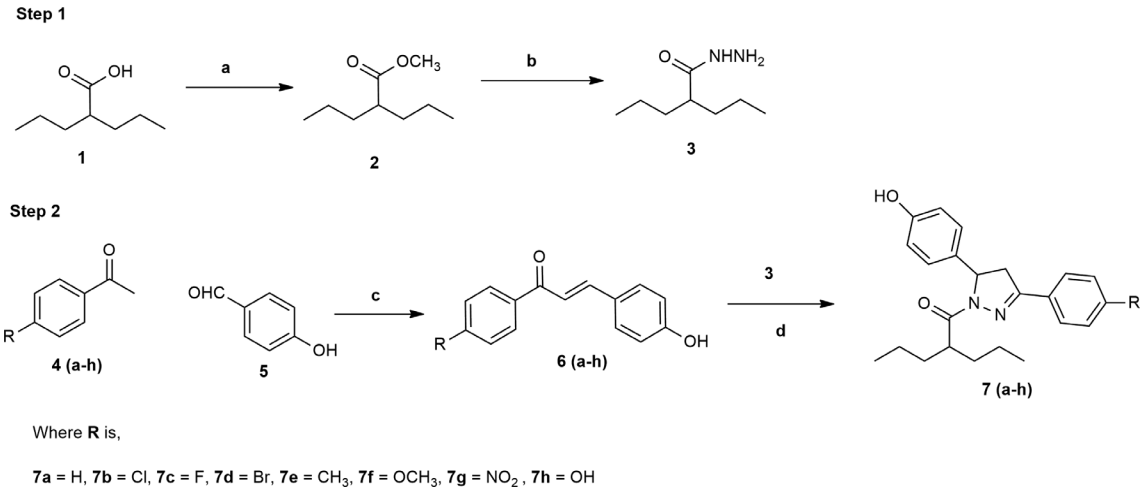

SCHEME 1 Synthesis of valproic acid-pyrazole derivatives **7(a-h)**. Reagents and conditions (a) methanol, H_2SO_4, 60–70°C (b) NH_2-NH_2, 110°C (c) NaOH, stirring for 24 h. (d) Ethanol, NaOH, reflux for 14–15 h, 100°C

TABLE 1 Antibacterial activity of valproic acid-pyrazole conjugates **7** (**a–h**)

	MIC, µg/ml			
Compound	***P. gingivalis***	***P. intermedia***	***F. Nucleatum.***	***E. coli***
7a	32	32	8	16
7b	1	1	1	4
7c	0.5	0.5	0.5	0.25
7d	2	1	1	4
7e	4	1	1	2
7f	8	8	8	8
7 g	4	4	4	4
7 h	16	8	8	16
Cefixime	0.02	0.02	0.02	0.02

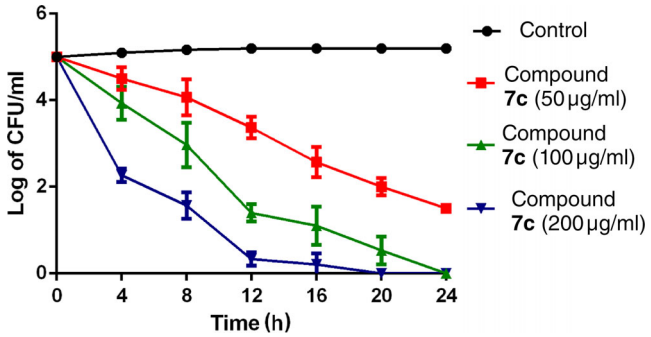

FIGURE 1 Time-kill curve of compound **7c** against *E. coli* showing bactericidal activity

TABLE 2 Inhibitory activity of compound **7c** on NF-κB transcriptional activity in LPS-stimulated RAW264.7 cells

Compound	**IC_{50}, in µM[a]**
7c	19.23 ± 2.11*
Control	0.85 ± 0.12
LPS	4.87 ± 1.31**
Dexamethasone (reference)	0.92 ± 0.48

[a]IC_{50} values expressed as mean ± SD of at least three independent assays. *P < .01 versus LPS, **P < .01 versus control.

results have been presented in Table 1. It has been found that compound **7a** exert the least activity among the tested derivative against all the bacterial organisms. However, the activity was significantly boosted against all the organisms in the case of compound **7b**. In the next instance, the activity was further increased against all the bacterial organisms, **7c**. The compounds **7d** and **7e** showed significant to mild activity in all the tested pathogens. Moreover, the antibacterial activity was further reduced considerably in the case of the rest of the compounds (**7f** and **7g**) with the least activity shown by **7h**. The antibacterial results revealed that none of the synthesized compounds showed activity comparable to cefixime as standard. However, they showed a diverse range of inhibitory activity suggesting compound **7a** as the least active molecule and compound **7c** as the most potent molecule among the tested series. The antibacterial results corroborated that, structural variation has a significant impact on the inhibitory activity such as, compound with no substitution showed the least inhibitory activity among the tested derivative (**7a**). Moreover, the compounds with substitution showed with significant antibacterial activity (**7b**, **7c**, **7d**, **7e**, **7f**, **7 g**, and **7 h**). Among the substituted compounds, the presence of the electron-withdrawing group (e.g., Cl, F and Br, except NO_2) showed significant inhibitory activity while compounds with electron-donating substituent (OCH_3, CH_3, OH) showed marginal loss in antibacterial activity. These results were found in agreement with the previous studies where the antibacterial activity was markedly improved in the case of electron withdrawing substituent [Srivastava, Dubey, et al., 2015; Singh et al., 2014; Singh et al. 2012b] .

Prompted by the exceptional antibacterial activity of compound **7c** against the tested bacterial organisms, it is worthwhile to determine its minimum bactericidal concentration (MBC) against these pathogens. The MBC is defined as the minimum concentration needed to kill ≥99.9% (≥3 log10) of the viable organisms after 24-h incubation relative to the starting inoculums [Chikezie, 2017]. As

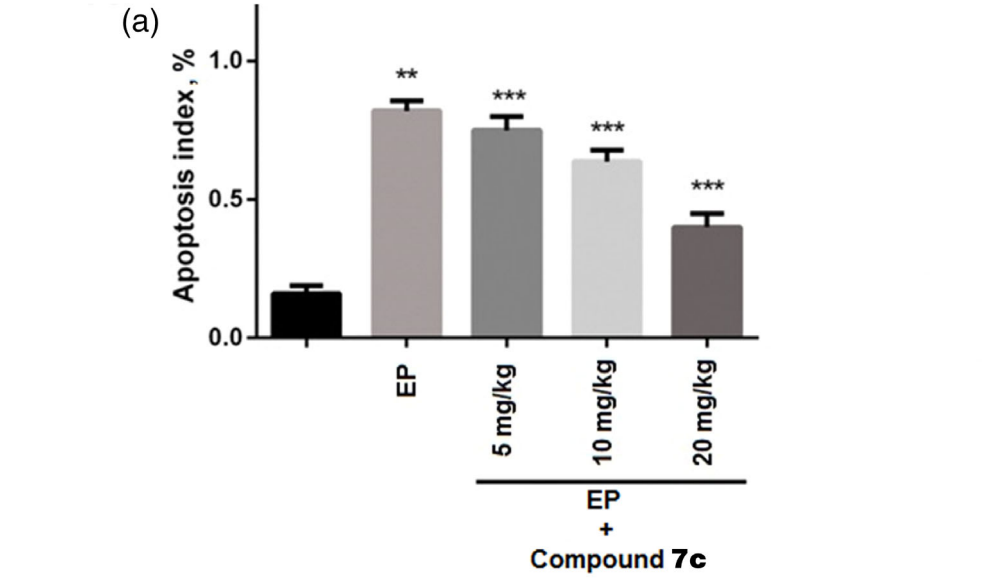

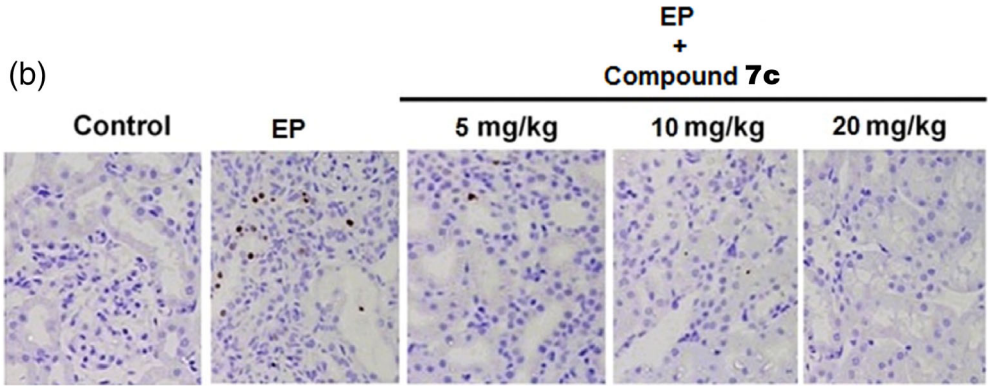

FIGURE 2 Effect of compound **7c** on the apoptosis after EP in rats (a) apoptosis index and (b) TUNEL staining. Values represent the mean ± SEM. $^{**}P < .05$ versus control; $^{***}P < .05$ versus EP group, one-way ANOVA followed by Bonferroni post hoc test

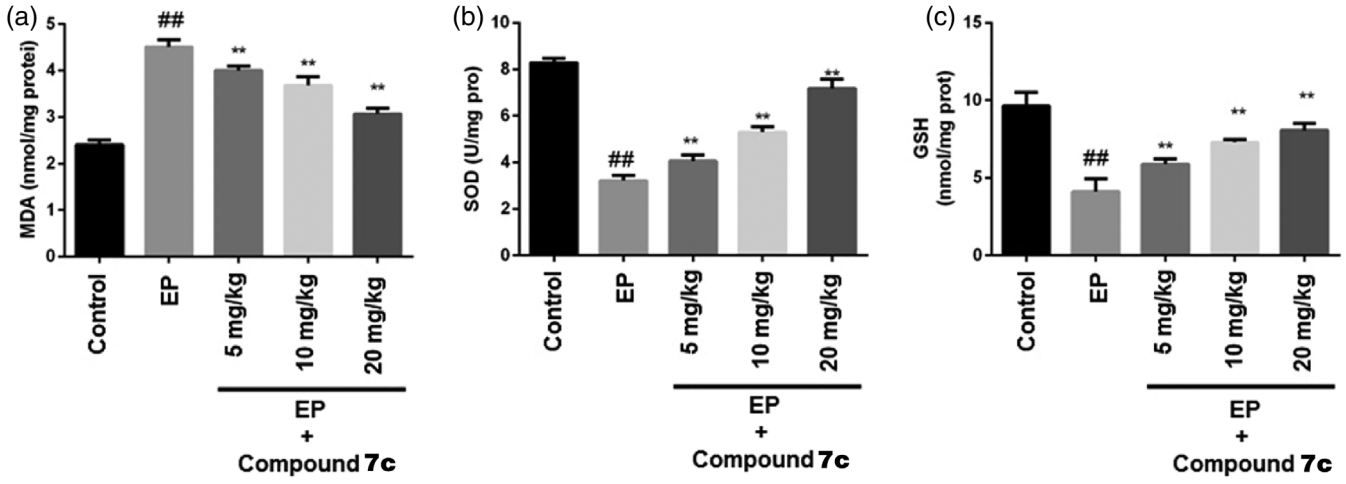

FIGURE 3 Effect of 7c on the oxidative stress in injury in rats (a) MDA, (b) SOD, and (c) GSH. Values represent the mean ± SEM. $^{**}P < .05$ versus control; $^{***}P < .05$ versus EP group, one-way ANOVA followed by Bonferroni post hoc test

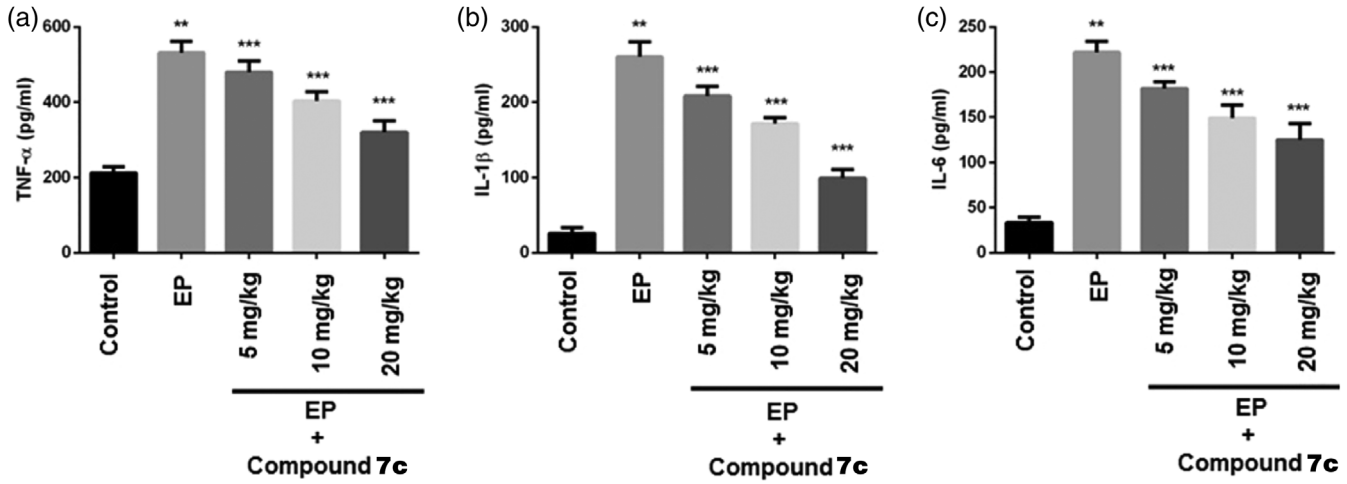

FIGURE 4 Effect of compound 7c on pro-inflammatory cytokines (a) TNF- α, (b) IL-1β, and (c) IL-6. Values represent the mean ± SEM. $^{**}P < .05$ versus control; $^{***}P < .05$ versus EP group, one-way ANOVA followed by Bonferroni post hoc test

shown in Figure 1, in a time-kill assay, compound **7c** showed exceptional bactericidal activity. It has been found that compound **7c** at the concentration of 100 and 200 μg/ml showed complete killing of *E. coli* at the 20 and 24 h, respectively.

3.3 | In vitro NF-κB transcription inhibitory activity of compound 7c

Nuclear factor-kappa B (NF-κB) belongs to a member of the transcription factor family. Various studies have implicated the role of NF-κB in synchronizing the expression of various genes in the inflammatory cascade of periodontitis. The activation of NF-κB by stimuli, such as tumor necrosis factor-α (TNF-α), interleukin-1β (IL-1β), IL-6, reactive oxygen intermediates (ROIs), receptor activator NF-κB ligand, ultraviolet irradiation, lipopolysaccharide (LPS), and other bacterial and viral agents. After activation, it triggers the release of cytokines that regulate the immune response, as well as adhesion molecules, which lead to the recruitment of leukocytes to sites of inflammation [Srivastava, Awatade, et al., 2015]. Thus, inhibition of NF-κB proved beneficial in controlling the inflammation of periodontitis. In the present study, the effect of compound **7c** was investigated on inhibitory effect on NF-κB transcriptional activity in LPS-stimulated RAW264.7 cells, where it showed excellent inhibition, Table 2.

3.4 | Effect of 7c on the cellular apoptosis of gingival tissues

To assess whether **7c** has any anti-apoptotic activity, TUNEL staining was performed and results are presented in Figure 2. It has been found that TUNEL positive cells were increased after the injury as compared to control. Upon administration of **7c**, the TUNEL positive cells were decreased significantly in a dose-dependent manner as compared to the EP group. These results were further elaborated by apoptosis index where compound **7c** reduces apoptosis index as compared to control.

3.5 | Effect of 7c on oxidative stress

The effect of compound **7c** was also quantified on the indices of oxidative stress and results have been presented in Figure 3. The control group showed no indication of oxidative stress. However, in EP group the level of oxidative stress has been elevated following the injury, as evidenced by a reduced level of MDA and increased level of SOD and GSH. However, upon administration of **7c**, the level of these oxidative stress biomarkers was restored significantly near to normal in a dose-dependent manner.

3.6 | Effect of compound 7c on inflammatory markers

The effect of compound **7c** was studied on various pro-inflammatory cytokines. As shown in Figure 4 the level of these cytokines (TNF-α, IL-1β, and IL-6) were found significantly elevated in the EP group as compared to the control. Furthermore, on the administration of **7c**, the level of these tested cytokines was found significantly reduced in a dose-dependent manner.

3.7 | Effect of compound 7c on COX-2 and iNOS

In the next instance, the effect of **7c** was investigated on the expression of COX-2 and iNOS to explore its possible mechanism of action against injury via western blot analysis. As shown in Figure 5, the level of COX-2 and iNOS was found elevated significantly in the EP group as compared to the control. Moreover, after administration of compound **7c** the level of these inflammatory (COX-2 and iNOS) was reduced significantly in a concentration-dependent manner.

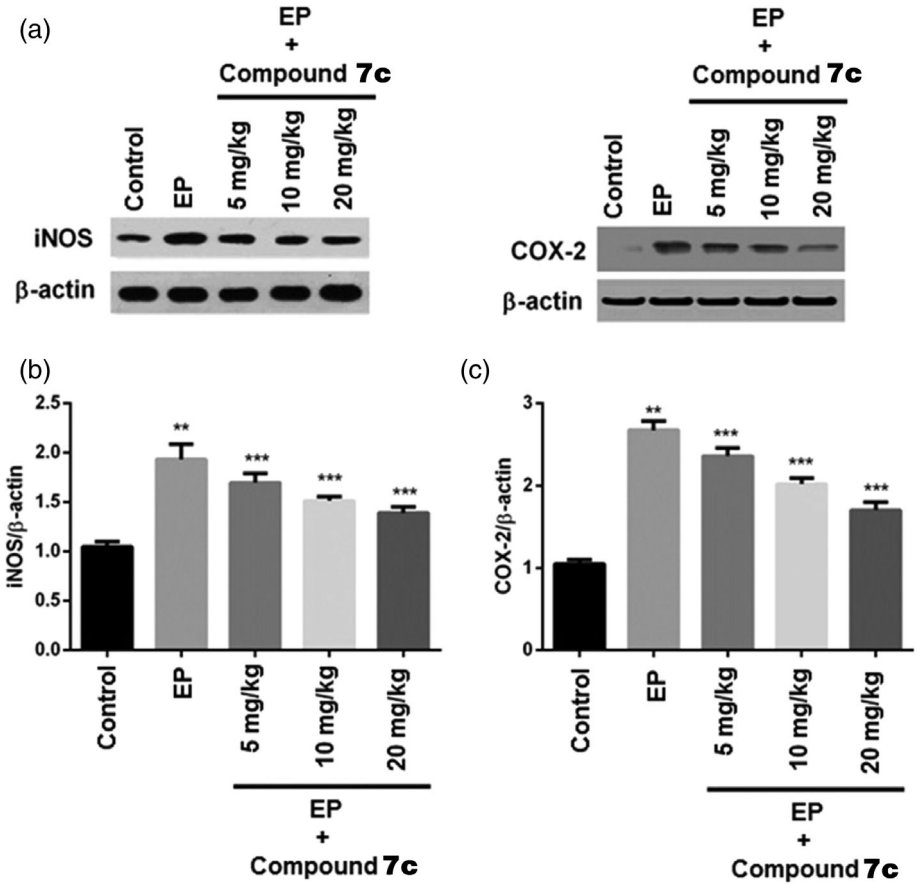

FIGURE 5 Effect of compound 7c on the expression of (a) COX-2 and iNOS by western blot, (b) qualitative bar graph showing the expression of COX-2, and (C) iNOS. Values represent the mean ± SEM. $^{**}P < .05$ versus control; $^{***}P < .05$ versus EP group, one-way ANOVA followed by Bonferroni post hoc test

4 | CONCLUSION

In summary, the results of the current study suggest the protective effect of compound **7c** against periodontitis via inhibition of inflammation, oxidative stress, and apoptosis. It also causes inhibition of COX-2 and iNOS for possible strong anti-inflammatory effects.

ACKNOWLEDGMENT

This study was supported by Quality Engineering Projects in Anhui Province: A High-Level Teaching Team of Stomatology (No: 2018jxtd103).

DATA AVAILABILITY STATEMENT

The data that support the findings of this study are available from the corresponding author upon reasonable request.

ORCID

Lei Dong https://orcid.org/0000-0001-2345-6789

REFERENCES

Ansari, A., Ali, A., Asif, M., & Shamsuzzaman. (2016). Review: Biologically active Pyrazole derivatives. *New Journal of Chemistry*, *41*(1), 16–41.

Cekici, A., Kantarci, A., Hasturk, H., & van Dyke, T. E. (2014). Inflammatory and immune pathways in the pathogenesis of periodontal disease. *Periodontology*, *64*(1), 57–80.

Chateauvieux, S., Morceau, F., Dicato, M., & Diederich, M. (2010). Molecular and therapeutic potential and toxicity of Valproic acid. *Journal of Biomedicine and Biotechnology*. https://doi.org/10.1155/2010/479364.

Chikezie, I. O. (2017). Determination of minimum inhibitory concentration (MIC) and minimum bactericidal concentration (MBC) using a novel dilution tube method. *African Journal of Microbiology Research*, *11*(23), 977–980.

Hajishengallis, G. (2015). Periodontitis: From microbial immune subversion to systemic inflammation. *Nature Reviews Immunology*, *15*(1), 30–44.

Karrouchi, K., Radi, S., Ramli, Y., Taoufik, J., Mabkhot, Y. N., Al-Aizari, F. A., & Ansar, M. (2018). Synthesis and pharmacological activities of Pyrazole derivatives: A review. *Molecules*, *23*(1), 134–187.

Khan, M. F., Alam, M. M., Verma, G., Akhtar, W., Akhter, M., & Shaquiquzzaman, M. (2016). The therapeutic voyage of Pyrazole and its analogs: A review. *European Journal of Medicinal Chemistry*, *14*(120), 170–201.

Li, X., Kolltveit, K. M., Tronstad, L., & Olsen, I. (2000). Systemic diseases caused by Oral infection. *Clinical Microbiology Reviews*, *13*(4), 547–558.

Parekh, S. P. (2010). *Synthesis and characterization of pharmacologically active compounds*. Saurashtra University.

Phiel, C. J., Zhang, F., Huang, E. Y., Guenther, M. G., Lazar, M. A., & Klein, P. S. (2001). Histone deacetylase is a direct target of Valproic acid, a potent anticonvulsant, mood stabilizer, and teratogen. *Journal of Biological Chemistry*, *276*(39), 36734–36741.

Singh, B., Bhat, H. R., Kumawat, M. K., & Singh, U. P. (2014). Structure-guided discovery of 1,3,5-Triazine-Pyrazole conjugates as antibacterial and Antibiofilm agent against pathogens causing human diseases with favorable metabolic fate. *Bioorganic and Medicinal Chemistry Letters*, *24*(15), 3321–3325.

Singh, U. P., Pathak, M., Dubey, V., Bhat, H. R., Gahtori, P., & Singh, R. K. (2012). Design, synthesis, antibacterial activity, and molecular docking studies of novel hybrid 1,3-Thiazine-1,3,5-Triazine derivatives as potential bacterial translation inhibitor. *Chemical Biology and Drug Design*, *80*(4), 572–583.

Srivastava, J. K., Awatade, N. T., Bhat, H. R., Kmit, A., Mendes, K., Ramos, M., Amaral, M. D., & Singh, U. P. (2015). Pharmacological

evaluation of hybrid Thiazolidin-4-One-1,3,5-Triazines for NF-κB, biofilm and CFTR activity. *RSC Advances*, *5*(108), 88710–88718.

Srivastava, J. K., Dubey, P., Singh, S., Bhat, H. R., Kumawat, M. K., & Singh, U. P. (2015). Discovery of novel 1,3,5-Triazine-Thiazolidine-2,4-Diones as dipeptidyl Peptidase-4 inhibitors with antibacterial activity targeting the S1 pocket for the treatment of type 2 diabetes. *RSC Advances*, *5*, 14095–14102.

Wade, W. G. (2012). The Oral microbiome in health and disease. *Pharmacological Research*, *18*(2), 109–120.

Zutz, C., M. Bacher, A. Parich, B. Kluger, A. Gacek-Matthews, R. Schuhmacher, M. Wagner, K. Rychli, and J. Strauss. 2016. "Valproic acid induces antimicrobial compound production in Doratomyces microspores." *Frontiers in Microbiology*, *7*(510). https://pubmed.ncbi.nlm.nih.gov/27148199/.

SUPPORTING INFORMATION

Additional supporting information may be found online in the Supporting Information section at the end of this article.

How to cite this article: Dong, L., Fang, L., Dai, X., Zhang, J., Wang, J., & Xu, P. (2021). Antibacterial and anti-inflammatory activity of valproic acid-pyrazole conjugates as a potential agent against periodontitis. *Drug Development Research*, 1–11. https://doi.org/10.1002/ddr.21851